JOURNAL OF MATERIALS SCIENCE 23 (1988) 1131–1136

Surface polarity and symmetry in semiconducting compounds

Part 1 *Macroscopic effects of polarity*

D. B. HOLT
Department of Metallurgy and Materials Science, Imperial College of Science and Technology, London SW7 2BP, UK

The polarity of the crystallographic surfaces of semiconducting compounds with the sphalerite and wurtzite structures results in gross differences in macroscopic chemical, mechanical and crystal growth behaviour which are reviewed. The asymmetry of the orthogonal $\langle 1\,1\,0 \rangle$ directions in $\{1\,0\,0\}$ surfaces of sphalerite structure materials is manifested in phenomena arising from $\{1\,1\,1\}$A–$\{\bar{1}\,\bar{1}\,\bar{1}\}$B differences. To treat these phenomena the surface polarity index and the singular surface polyhedra for sphalerite- and wurtzite-structure semconducting compounds are introduced.

1. Introduction

The adamantine (diamond-like) semiconducting compounds and alloys are partially ionic and it has been argued that the degree of ionicity of binary compounds determines whether the crystal structure adopted is sphalerite or wurtzite [1]. The polarity of these structures was early found to result in large differences in macroscopic surface properties, reflecting the symmetry of the crystal structures involved.

The ionicity and surface polar symmetry of these materials were also suggested to have a controlling influence in epitaxial growth. For example the polarity of substrate surfaces can determine the structure, sphalerite or wurtzite, of epitaxial II–VI films [2] and the polarity of substrate surfaces tends to be continued in the epitaxial films [3]. The orientation (symmetry) of the surfaces of diamond structure substrates similarly determines the structure of epitaxial II–VI films in many cases [4]. It has also been argued that the ionicity of compound substrates can be used to predict the structures of epitaxial films of polymorphic semiconducting compounds [5].

The polar surface properties of sphalerite and wurtzite structure materials have not been reviewed so this is done in the present paper which also introduces a polarity index and polar singular surface polyhedra to aid in treating surface polarity. In a second paper more powerful dichromatic symmetry group methods will be introduced and the role of symmetry and polarity in epitaxy will be discussed.

2. Macroscopic differences between polar faces in sphalerite and wurtzite structure semiconductors

The sign convention for polarity used here is that most widely employed for compounds with an AB atom pair at the points of the space lattice [6]. The A atom is that of the lower valence, e.g. the III valent element in a III–V compound. For mnemonic convenience, the A (alabaster) element sites will be represented by white circles and the B element by black ones. The polar sign convention places A atoms on the lattice sites, e.g. that at the origin, and B atoms at the other sites of the basis unit, e.g. at 1/4, 1/4, 1/4 in the cubic unit cell of the sphalerite structure. The covalent bonds are polar and the $[1\,1\,1]a$ direction is that from the A atom to the B atom to which it has a $[1\,1\,1]$ bond. Similarly, in the wurtzite structure, the A atoms are placed on the lattice sites and $[0\,0\,0\,1]a$ is the direction from an A atom to the B atom to which it has an $[0\,0\,0\,1]$ oriented bond as shown in Fig. 1. On this convention, introduced by Gatos, the A faces are indexed, like $(1\,1\,1)$, with an even number of negative indices and B faces, like $(\bar{1}\,\bar{1}\,\bar{1})$, with an odd number of negative indices. Many papers, following the earlier work of Dewald [17], use the opposite convention, so care must be exercised in following the literature.

The polar directions $[1\,1\,1]a$ and $[0\,0\,0\,1]a$ can be determined by X-ray diffraction methods [7–15]. The polarity of the faces to which, for example, the $[1\,1\,1]a$ and $[\bar{1}\,\bar{1}\,\bar{1}]b$ directions are the outward normals, are then assumed, on energetic grounds, to be of the $(1\,1\,1)$A type, consisting of triply bonded A atoms and $(\bar{1}\,\bar{1}\,\bar{1})$B (triply bonded B surface atom) type, respectively, as illustrated in Fig. 1a. Similarly, in the wurtzite structure the $[0\,0\,0\,1]a$ direction is the outward-drawn normal to what is assumed to be the $(0\,0\,0\,1)$A face consisting of triply bonded A atoms, etc.

The experimental evidence that this assumption is correct is that of Brongersma and Mul [16] using noble ion reflection mass spectroscopy (also known as ion scattering spectroscopy, ISS). They determined the bulk, directional polarity in sphalerite-structure ZnS and in wurtzite-structure CdS using X-rays. The outermost atomic layers of the polar surfaces were then "mass analysed" by determining the incident-ion energy loss on back scattering from atomically clean surfaces in ultra-high vacua. This showed that the

0022–2461/88 $03.00 + .12 © *1988 Chapman and Hall Ltd.*

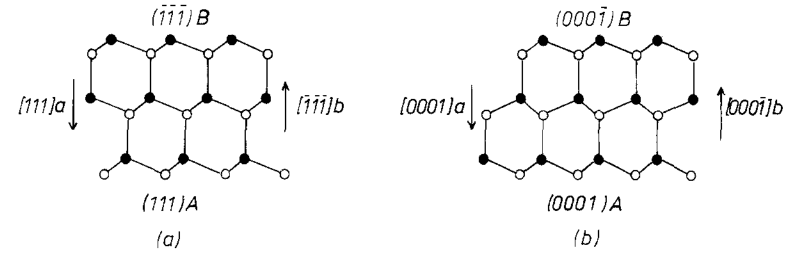

Figure 1 Polarity in (a) the sphalerite and (b) wurtzite structures. For mnemonic convenience, in AB compounds, e.g. III–V or II–VI, the B atoms are black and the A atoms are alabaster (white).

(1 1 1) and (0 0 0 1) faces as defined by X-ray diffraction and etching were A faces, i.e. consisted predominantly of zinc and cadmium surface atoms, respectively. The $(\bar{1}\,\bar{1}\,\bar{1})$ and $(0\,0\,0\,\bar{1})$ faces consisted predominantly of sulphur surface atoms in both cases, i.e. were of B type. It is desirable that the polar character of atomically clean surfaces be checked using Rutherford back scattering and other methods on additional materials.

2.1. Chemical and crystal growth differences

Dewald [17] initiated research on semiconductor surface polarity by studying the rate of anodic oxidation as a function of the surface orientation of InSb. This and subsequent work showed that the (1 1 1)A faces of III–V compounds are more noble (less reactive) than the $(\bar{1}\,\bar{1}\,\bar{1})$B faces.

Practical interest resulted from the early observations that the polarity of the {1 1 1} surfaces strongly affected the chemical etching [18–20] and crystal growth behaviour [21, 22] of sphalerite-structure III–V compounds. It was found that the more reactive $(\bar{1}\,\bar{1}\,\bar{1})$B faces of III–V compounds were more rapidly dissolved in oxidizing reagents and tended to develop smooth polished surfaces. The less reactive (1 1 1)A faces dissolved more slowly and could be made to exhibit dislocation etch pits [9, 10, 19]. Etch inhibitors had to be used to make etch pits visible on the faster-attacked $(\bar{1}\,\bar{1}\,\bar{1})$B faces [23]. The principles involved are covered by reviews [24, 25]. Electrochemical tunnel etching occurs in the $\langle 1\,1\,1\rangle a$ directions, from gallium to phosphorus in GaP [26] and gallium to arsenic in GaAs [27, 28]. Polar etching behaviour in many II–VI compounds were reported by Warekois *et al.* [29]. In Czochralski crystal growth in $\langle 1\,1\,1\rangle$ directions, better crystals were more consistently obtained if the seed was inserted with a (1 1 1)A face down [21, 30, 31]. The autoradiographic studies of segregation in the growth of InSb provided evidence that (1 1 1)In facets were more readily eliminated from convex-solid/liquid interfaces during growth than were $(\bar{1}\,\bar{1}\,\bar{1})$Sb facets. It was suggested that this is responsible for the polarity of the frequency of twinning during growth in the $\langle 1\,1\,1\rangle$ directions [32].

Differences in contact alloying behaviour [33, 34] and temperature of surface thermal decomposition [35, 36] were also found between faces of opposite polarity.

2.2. Differences in mechanical properties

Contemporary interest in dislocations and mechanical properties drew attention to the polar differences in surface damage and consequent effects. When {1 1 1} slices of InSb were mechanically polished down to thicknesses of about 10 μm, they spontaneously bent. The wafers always had the (1 1 1)A(In) face on the concave side [37]. That the curling of mechanically thinned slices was due to differences in subsurface damage was proved by Haneman [38]. He measured the curvature of slices mechanically polished on one side and etched and damage-free on the other. They were all concave on the etched side, whether this was of (1 1 1)In or $(\bar{1}\,\bar{1}\,\bar{1})$Sb polarity. The strain energy in the damaged surface was found to be about $10^{-3}\,\mathrm{J\,m^{-2}}$. The difference in subsurface damage strain responsible for the curvature of slices mechanically polished from both sides is about 10^{-3} of this value and the strain is larger on the B side.

There are small inherent differences in surface tension between A and B faces. Ion-bombardment thinned and annealed wafers of InSb and GaSb, 10 to 20 μm thick were examined in ultra-high vacuum. They had curvatures below the detection limit of a laser interferometer. This gave an upper limit of $4 \times 10^{-1}\,\mathrm{N\,m^{-1}}$ for the difference in surface tension between the A and B faces of these compounds [39]. Crystals of AlN grown as blades with thicknesses of the order of 10^2 nm were found by transmission electron microscopy to be spontaneously bent. The observations gave a difference in surface tension between the polar {1 1 1} surfaces of $3.63 \pm 0.15\,\mathrm{N\,m^{-1}}$ [40]. Both these values are consistent with theoretical calculations of surface tensions from the elastic constants [41].

Polar differences in surface hardness were found in BeO and other wurtzite-structure compounds [42]. Polar differences in cleavage morphology were observed in a wide range of adamantine semiconductors [43, 44].

The piezoelectric stress constants of a number of III–V compounds were measured. The results showed that in all of them the (1 1 1)A faces have negative charges when the compounds are expanded in the [1 1 1] direction [45]. The sign of charge developed in II–VI compounds with the same sphalerite structure under the same [1 1 1] tensile strain is the opposite of this. That is, in the II–VI compounds, the (1 1 1)A faces then develop positive charges [46]. In the case of wurtzite-structure BeO it was established that both the pyroelectric and piezoelectric effects result in a negative charge on the (0 0 0 1)O face under compression [47]. The surface charge on anodized InSb was found to be orientation dependent [48] and polarity was reported to affect energy band bending at Cs_2O-activated surfaces of GaAs [49].

2.3. [1 1 0]–$[\bar{1}\,1\,0]$ differences in (0 0 1) surfaces

The other low-index surface orientation in which

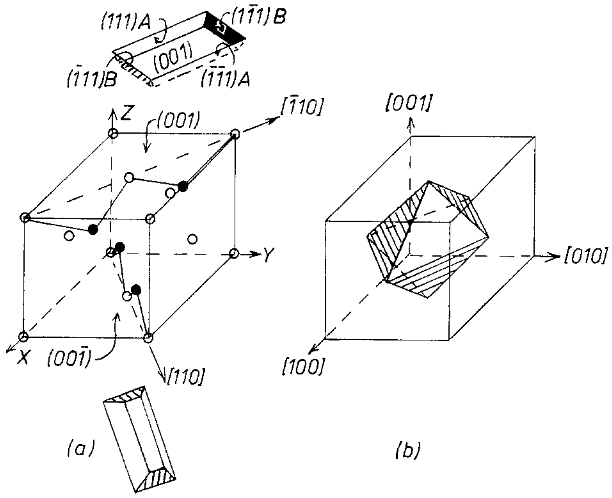

Figure 2 $[\bar{1}10]$–$[110]$ dissimilarities in $\{001\}$ surfaces (a) in a unit cell – the $[\bar{1}10]$ direction is bonded down into the interior of the (001) face whereas the $[110]$ direction is bonded up into the $(00\bar{1})$ face. Etch pits in an (001) face are elongated in the $[\bar{1}10]$ direction because the $\{\bar{1}\bar{1}\bar{1}\}$B faces are rapidly attacked, whereas the less reactive $\{111\}$A faces recede more slowly. This results in orthogonally aligned pits on the top and bottom surfaces of $\{001\}$ slices of sphalerite structure materials. (b) The polar octahedron gives the relative orientations of all the outward-facing $\{111\}$A and $\{\bar{1}\bar{1}\bar{1}\}$B faces. Cross-hatching here indicates black (B) facets seen through another surface in the diagram.

polar differences have been reported is $\{001\}$. These are not differences between $\{001\}$ faces but between the two orthogonal $\langle 110\rangle$ directions in these faces. The $[110]$ and $[\bar{1}10]$ directions in the $\{001\}$ faces are crystallographically distinct as seen in Fig. 2a.

The pits produced by the Sirtl etch [50] on the two opposite sides of $\{001\}$ slices of GaAs were found to be elongated in $\langle 110\rangle$ directions at right angles to each other [51]. Consequently [51, 52] such etch pits can be used to differentiate the $[110]$ and $[\bar{1}10]$ type directions in (001) faces. Thermal decomposition in vacuum also results in pits elongated along the orthogonal $\langle 110\rangle$ directions on opposite faces of $\{001\}$ slices of InP [53, 54]. The form and orientation of the pits are shown in Fig. 2a. The direction of elongation of the pits is determined by the chemical character of the $\{111\}$ faces: the more reactive, higher energy B faces, e.g. $(\bar{1}\bar{1}\bar{1})$, are more rapidly attacked or more rapidly decomposed and so recede faster, while the lower-energy A faces, e.g. (111), recede more slowly. The long axis of the pits on the (001) face is, therefore, aligned with the $[\bar{1}10]$ direction and the short with $[110]$. (Confusion can arise because these directions and planes are oppositely indexed, following the Dewald convention, in half the papers in this field [53, 54].) The crossed alignment of the pits on the upper (001) and lower $(00\bar{1})$ faces of a $\{001\}$ slice are illustrated above and below the conventional structure cell in Fig. 2. The polar octahedron of $\{111\}$ surfaces [6] is useful in this context. The pits are bounded by facets converging down into the $\{001\}$ surface and corresponding to the faces of the octahedron nearer to the surface. (The faces of the octahedron are coloured to represent the polarity of the outward facing planes.) It can be seen in Fig. 2 that this enables one to determine the pit orientations on alternative faces of the cubic structure cell.

Defects formed in (001) hetero-epitaxial layers also often exhibit dissimilarities in the orthogonal $\langle 110\rangle$ directions. This will be dealt with in a subsequent paper [55].

2.4. The shapes of etch pits on twinned $\{111\}$ faces

Durose [56, 57] analysed first-, second- and third-order twins in vapour-phase grown boules of CdTe. On planar surfaces corresponding to $\{111\}$ surfaces of the matrix, the twinned areas have surface orientations such as $\{5\bar{1}\bar{1}\}$ for the first order and $\{5\bar{7}13\}$ for the second order. Durose accounted for the complex shapes of the etch pits on these faces by noting that the facets of the pits were of $\{\bar{1}\bar{1}\bar{1}\}$Te polarity. The intersection of the surface plane with the polar $\{\bar{1}\bar{1}\bar{1}\}$Te tetrahedron then gives the observed pit shapes.

3. The polarity index and polar singular surface polyhedra

Means for quantitatively specifying the degree of polarity of a surface and for visualizing the crystallographic relations of the singular orientations and their polarity are sometimes needed.

3.1. Polarity indices

The relative polarity of any face in a binary AB compound can be specified by a polarity index defined to be

$$P = (n_A - n_B)/n_T \qquad (1)$$

where n_A, n_B and n_T are the numbers of A, B and the total of all atoms $n_T = n_A + n_B$ in a unit mesh or unit area of the surface. $P = 1$ and -1 represent the polarities of fully polar faces of opposite sign such as the $\{111\}$A and $\{\bar{1}\bar{1}\bar{1}\}$B faces of the sphalerite structure represented in the polar octahedron [6]. $P = 0$ indicates a fully non-polar (neutral) surface, which would be of zero intrinsic net charge in an atomically clean unreconstructed state on an ionic crystal. Non-integral values of P indicate partial polarity. Orientations for which $0 < P < 1$ contain a preponderance of surface A atoms. If $-1 < P < 0$, the face is predominantly surfaced with B atoms. Polyhedra can be drawn to represent the surface orientations of given polarities as the polar octahedron represented the $P = 1$ and -1 orientations in the sphalerite structure [6].

3.2. Singular and vicinal surfaces

Singular surfaces are defined by energetic, etching and growth-rate considerations [58]. Suppose that the relative etching rates for all surface orientations are determined by studies of spheres cut from single crystals of a given material. Let these rates be represented by vectors drawn from a common origin. The locus of the ends of these vectors (Wulff plots) constitute what Frank terms "raspberry figures". Concave cusps in these surfaces define the minimal etch rate vectors. These vectors are normal to surface

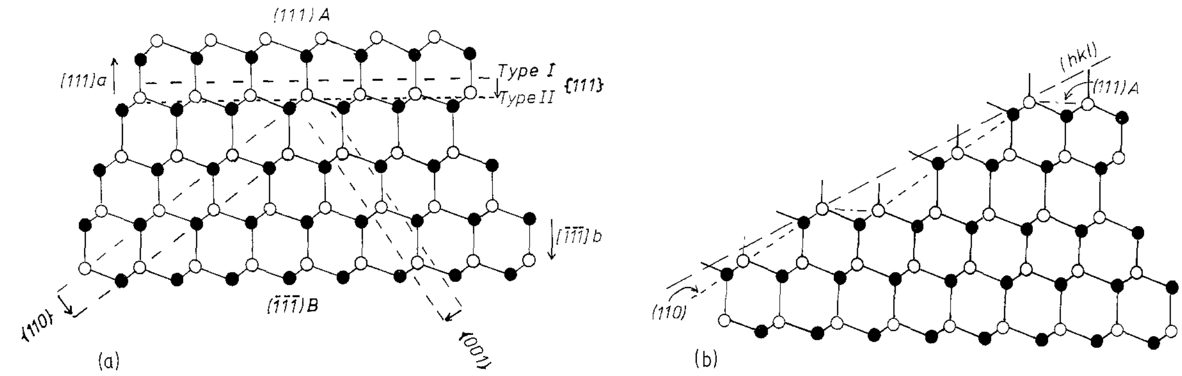

Figure 3 (a) Singular surface orientations in the sphalerite structure correspond to high atom density crystallographic planes. There are {1 1 1} and {1 1 0} planes normal to the plane of the figure and a {1 0 0} plane inclined to the plane of the diagram as shown. The type I {1 1 1} plane cuts one bond per atom and has a {1 1 1}A face below. The type II {1 1 1} plane cuts three bonds per atom and has an unstable B face below. The two {1 1 0} planes are equivalent. The two {1 0 0} planes each cut two bonds per atom although this is not obvious in this projection of the crystal structure. One has a {1 0 0}A face and the other a {1 0 0}B face below it. (b) A vicinal free surface in the sphalerite structure, which can be resolved into relatively wide (0 1 1) facets and (1 1 1)A atomic steps.

orientations of minimal energy and reactivity. These are the singular surfaces and those of nearby orientations are the related vicinal (atomically stepped) surfaces.

Geometrically, singular crystallographic surfaces are those for which all the surface atoms, i.e. those with cut bonds or missing nearest neighbours can lie in a single geometrical plane as can be seen in Fig. 3a for the case of the sphalerite structure. On vicinal surfaces, the atoms with cut bonds do not all lie in a plane. Vicinal surfaces can, therefore, be resolved into atomic-scale singular surface facets as illustrated in Fig. 3b.

An important distinction is that between steps and "demi-steps" (Pond [59]). Complete steps lead from one planar area to another parallel one, both of the same polarity. Demi-steps connect parallel facets of opposite polarity. The height of complete steps is given by

$$h_c^s = \boldsymbol{n} \cdot \boldsymbol{t}_i \qquad (2)$$

where $\boldsymbol{n}$ is the outward normal to the surface, and $\boldsymbol{t}_i$ is a lattice translation vector whereas demi-steps are of height

$$h_d^s = \boldsymbol{n} \cdot (\boldsymbol{t}_i + \boldsymbol{r}) \qquad (3)$$

where $\boldsymbol{r}$ is the vector joining the sites of the basis unit, i.e. $\boldsymbol{r} = 1/4\langle 1\,1\,1\rangle$ in the diamond and sphalerite structures.

3.3. The sphalerite singular surface polyhedron

The singular surface orientations in the sphalerite structure are {1 0 0}, {1 1 0} and {1 1 1} shown in Fig. 2. {1 1 1} surface planes can occur in $P = 1$, e.g. (1 1 1)A, and $P = -1$, e.g. $(\bar{1}\,\bar{1}\,\bar{1})$B forms [6] as shown in Fig. 1. {1 1 0} planes contain equal numbers of A and B atoms as can be seen in Fig. 2, so all {1 1 0} surface planes are exactly non-polar (neutral), i.e. $P = 0$. {1 0 0} planes contain all A or all B atoms. The case of {1 0 0} surfaces in the sphalerite structure requires a different form of discussion, suggested by Frank [60].

Let a planar surface in each of the singular orientations be passed through an array of atoms. Suppose the {1 1 1} plane to occupy an {1 1 1}A configuration, containing only A atoms triply bonded to the crystal. If it is translated in the direction normal to itself it will alternately pass through B atoms only and A atoms only. However, the B atom configurations are energetically untenable as free surfaces because the B atoms would be only singly bonded to the crystal. Hence the {1 1 1} orientation is necessarily polar. A {1 1 0} surface will contain equal numbers of A and B atoms, each doubly bonded to the crystal. Translating the {1 1 0} plane normal to itself will carry it through a succession of positions of which the preceeding statements are always true. Thus the {1 1 0} orientation is inherently exactly ($P = 0$) non-polar and it is of higher energy (two cut bonds per surface atom instead of one) than the {1 1 1} surfaces. {1 1 0} is the cleavage plane in the sphalerite structure because splitting along this plane does not result in the separation of electrostatically charged polar faces as cleavage along {1 1 1} planes would.

A {1 0 0} oriented planar surface can pass through a plane containing only A atoms, each doubly bonded to the crystal. Parallel translation carries such a surface through planes of B atoms all doubly bonded to the crystal alternating with similarly energetic A atom planes.

It can be argued that real surfaces which are not atomically planar over macroscopic areas will be different in the three cases. {1 1 1} surfaces for energetic reasons (numbers of cut bonds per atom) will have steps of basis unit height, i.e. complete steps, so that successive stepped areas will be of the same polarity. That is, the entire area will consist of planar, stepped areas that are all of {1 1 1}A polarity or all of $\{\bar{1}\,\bar{1}\,\bar{1}\}$B polarity. {1 1 0} can have steps between adjacent planar areas of any height because all vertically displaced configurations are of the same number of cut bonds per atom (namely 2) and polarity ($P = 0$). {1 0 0} surfaces, however, could have steps of basis unit height, keeping the polarity constant so the surface would be all {1 0 0}A or all {1 0 0}B. Alternatively, {1 0 0} surfaces could have demi-steps between flat facets so the polarity would alternate from $P = 1$

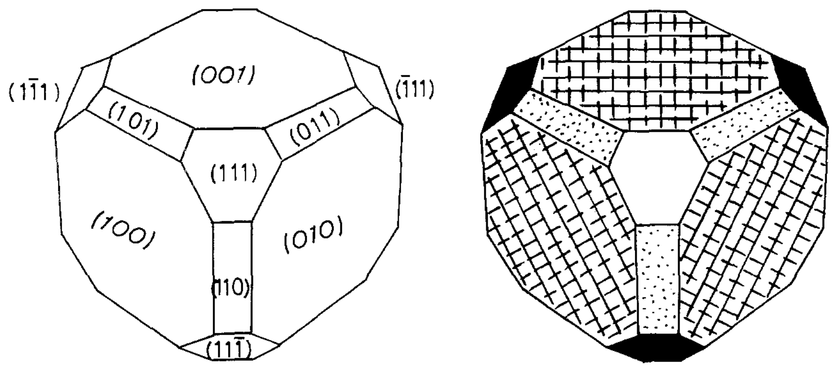

(a) (b)

Figure 4 The polar singular surface polyhedron of the sphalerite structure (a) with the faces indexed. (b) White and black indicate the A ($P = 1$) and B ($P = -1$) polarities, respectively, of the $\{1\,1\,1\}$ surfaces. The macroscopic $P \simeq 0$ polarity of the $\{1\,0\,0\}$ surfaces is represented by cross-hatching in the two non-equivalent, orthogonal $\langle 1\,1\,0\rangle$ directions in each $\{1\,0\,0\}$ plane. The $\{1\,1\,0\}$ non-polar faces are represented as grey (stippled), because they consist of equal numbers of A and B (black and white) atoms.

to -1. It is energetically favourable for the latter situation to prevail as surface electrostatic energy is minimized and the possibility of eliminating dangling bonds by connecting neighbouring bonds to form "right" A–B (strained) bonds are maximized. Sangster [61] first suggested that the $\{1\,0\,0\}$ faces of sphalerite structure materials would be non-flat on an atomic scale in this way on the basis of ball-and-wire crystal model studies related to crystal growth.

The experimental evidence is that to a first approximation, the $\{1\,0\,0\}$ surfaces like the $\{1\,1\,0\}$ surfaces are macroscopically non-polar. That is, no gross differences in etching, crystal growth behaviour, etc. have been reported between opposite faces of $\{1\,0\,0\}$ slices of sphalerite structure semiconductors. There are, however, the observations of asymmetries between the orthogonal $\langle 1\,1\,0\rangle$ directions in the $\{1\,0\,0\}$ plane noted above. The three types of surfaces are differentiated in the singular surface polyhedron for the sphalerite structure of Fig. 4, to indicate the difference between the inherent, exact non-polarity of the $\{1\,1\,0\}$ surfaces and the energetic, macroscopic non-polarity of $\{1\,0\,0\}$ surfaces made up of microscopic A and B stepped facets. The crosshatching by lines of different types is a reminder of the $\langle 1\,1\,0\rangle$ dissimilarity in $\{1\,0\,0\}$ surfaces.

3.4. The wurtzite singular surface polyhedron

The wurtzite structure is based on the hexagonal lattice with four atoms in the primitive hexagonal cell at positions with the coordinates, in terms of the lattice parameters a, a, c:

A atoms: $0, 0, 0$ (a site) and $2/3, 1/3, 1/2$ (b site)

B atoms: $0, 0, 1/2\text{-}u$ (α site) and $2/3, 1/3, 1\text{-}u$ (β site)

The labelling of the sites refers to the stacking sequence for close packed arrays, characteristic of the wurtzite structure: $a\,\alpha\,b\beta\,a\,\alpha\,b\beta\ldots$ The c/a ratio for wurtzite structure compounds is always close to the ideal hexagonal value of $(8/3)^{1/2}$. The value of u is always near to the ideal value for tetrahedral coordination of 3/8. The positions of the atoms in the hexagonal structure cell are shown in Fig. 5.

The common growth morphology of, for example, zincite (ZnO) and bromellite (BeO) with the wurtzite structure is of the form shown in Fig. 6 and is bounded by the $\{0\,0\,0\,1\}$ basal planes which are polar, $\{1\,0\,\bar{1}\,0\}$ prismatic planes and $\{1\,0\,\bar{1}\,1\}$ pyramidal planes. The prismatic planes contain the $\{0\,0\,0\,1\}$ direction connecting A to B atoms so they have polarity index $P = 0$. The pyramidal $(1\,0\,\bar{1}\,1)$ plane is sketched in Fig. 5 and is analogous to the $\{0\,0\,1\}$ planes in the sphalerite structure as can be seen by considering the adjacent atomic planes shown. Hence $P \simeq 0$ and faces of this form will be stepped to avoid polar charges and minimize the surface energy. The conclusions reached here are in accordance with the fact that only the $\{0\,0\,0\,1\}$ planes in wurtzite structure compounds exhibit macroscopic polarity effects. The polar singular surface polyhedron for the wurtzite structure therefore has the form shown in Fig. 6.

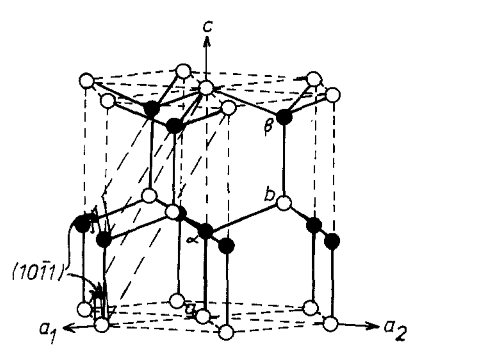

Figure 5 Atomic sites in the wurtzite structure. The sites marked a, α, b and β are those for which the coordinates, in the primitive hexagonal lattice unit cell with edges $\boldsymbol{a}_1$, $\boldsymbol{a}_2$ and $\boldsymbol{c}$, are listed in the text. The two adjacent atomic planes with the pyramidal orientation $(1\,0\,\bar{1}\,1)$ are analogous to the $\{0\,0\,1\}$ planes in Fig. 3(a) in that each contains atoms of one kind only, with similar numbers of cut bonds.

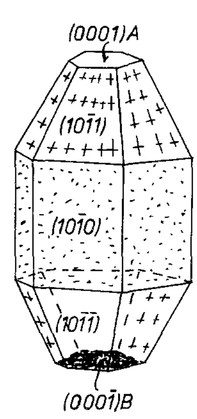

Figure 6 The singular surface polyhedron for the wurtzite structure. The polar character of the faces is indicated in the same way as in Fig. 4(b).

4. Discussion

The extensive literature briefly reviewed above shows that surface polarity has gross effects of the greatest practical importance. It is therefore useful to have means such as the sphalerite polar octahedron [6] or polar singular surface polyhedra for visualizing the crystallography involved in much the same way that Thompson's tetrahedron helps the visualization of the slip systems in fcc-lattice-based crystal structures. To treat surface polar symmetry and epitaxy, more powerful means such as dichromatic symmetry group theory is needed. This will be introduced and applied in a second paper [55].

Acknowledgements

It is a pleasure to thank Professor F. C. Frank and Dr R. C. Pond for helpful discussions.

References

1. P. LAWAETZ, *Phys. Rev.* **B5** (1972) 4039.
2. M. WEINSTEIN and G. A. WOLFF, in "Crystal Growth", Proceedings International Conference, Boston, edited by H. S. Peiser (Pergamon, Oxford, 1967) p. 537.
3. O. IGARASHI, *J. Appl. Phys.* **42** (1971) 4035.
4. D. B. HOLT, *Thin Solid Films* **24** (1974) 1.
5. K. HUBNER and G. KUHN, *Kristall. Technik.* **7** (1972) 1185.
6. D. B. HOLT, *J. Mater. Sci.* **19** (1984) 439.
7. D. COSTER, K. S. KNOL and J. A. PRINS, *Z. Physik* **63** (1930) 345.
8. R. W. JAMES, "The Optical Principles of the Diffraction of X-rays" (Bell, London, 1948) pp. 32–34.
9. J. G. WHITE and W. C. ROTH, *J. Appl. Phys.* **30** (1959) 946.
10. E. P. WAREKOIS and P. H. METZGER, *ibid.* **30** (1959) 960.
11. R. ZARE, W. R. COOK and L. R. SHIOZAWA, *Nature* **189** (1961) 217.
12. H. PFISTER, *Z. Naturforsch.* **16a** (1961) 427.
13. H. HOLLOWAY, *J. Appl. Phys.* **40** (1969) 2187.
14. K. F. BURR and J. WOODS, *J. Mater. Sci.* **6** (1971) 1007.
15. W. SCHMIDT, B. PILGERMANN, G. KUHN and P. FISHER, *Kristall. Technik.* **8** (1973) 913.
16. H. H. BRONGERSMA and P. M. MUL, *Chem. Phys. Lett.* **19** (1973) 217.
17. J. P. DEWALD, *J. Electrochem. Soc.* **104** (1957) 244.
18. H. C. GATOS and M. C. LAVINE, *ibid.* **107** (1960) 427.
19. J. W. ALLEN, *Phil. Mag.* **2** (1957) 1475.
20. H. C. GATOS and M. C. LAVINE, *J. Phys. Chem. Solids* **14** (1960) 169.
21. P. L. MOODY, H. C. GATOS and M. C. LAVINE, *J. Appl. Phys.* **31** (1960) 1696.
22. H. C. GATOS, P. L. MOODY and M. C. LAVINE, *ibid.* **31** (1960) 212.
23. H. C. GATOS and M. C. LAVINE, *ibid.* **31** (1960) 743.
24. J. W. FAUST, in "Semiconducting Compounds", Vol. 1, The Preparation of III–V Compounds, edited by R. K. Willardson and H. L. Goering (Reinhold, New York, 1962) pp. 445–68.
25. H. C. GATOS and M. C. LAVINE, *Prog. Semicond.* **9** (1964) 1.
26. B. D. CHASE and D. B. HOLT, *J. Electrochem. Soc.* **119** (1972) 314.
27. J. P. KRUMME and M. E. STRAUMANIS, *Trans. Met. Soc. AIME* **239** (1967) 395.
28. M. M. FACTOR, D. G. FIDYMENT and M. R. TAYLOR, *J. Electrochem. Soc.* **122** (1975) 1566.
29. E. P. WAREKOIS, M. C. LAVINE, A. N. MARIANO and H. C. GATOS, *J. Appl. Phys.* **33** (1962) 690.
30. K. F. HULME and J. B. MULLIN, *Solid State Electron.* **5** (1962) 211.
31. A. STEINMAN and U. ZIMMERLI, *ibid.* **6** (1963) 597.
32. J. B. MULLIN, in "Compound Semiconductors", Vol. 1, Preparation of III–V Compounds, edited by R. K. Willardson and H. L. Goering (Reinhold, New York, 1962) pp. 365–81.
33. M. T. MINAMOTO, *J. Appl. Phys.* **33** (1962) 1826.
34. E. L. HEASELL and H. D. BARBER, *Solid State Electron* **8** (1965) 176.
35. D. HANEMAN, in "Semiconducting Compounds", Vol. 1, Preparation of III–V Compounds, edited by R. K. Willardson and H. L. Goering (Reinhold, New York, 1962) pp. 432–5.
36. G. L. RUSSEL, H. K. IP and D. HANEMAN, *J. Appl. Phys.* **37** (1966) 3328.
37. R. E. HANNEMANN, M. C. FINN and H. C. GATOS, *J. Phys. Chem. Solids* **23** (1962) 1554.
38. D. HANEMAN, *Brit. J. Appl. Phys.* **16** (1965) 411.
39. A. TALONI and D. HANEMAN, *Surf. Sci.* **8** (1967) 323.
40. C. M. DRUM, *Phil. Mag.* **13** (1966) 1239.
41. J. W. CAHN and R. E. HANNEMANN, *Surf. Sci.* **1** (1964) 387.
42. C. F. CLINE and J. S. KAHN, *J. Electrochem. Soc.* **110** (1963) 773.
43. G. A. WOLFF and J. D. BRODER, *Acta Crystallogr.* **12** (1959) 313.
44. M. S. ABRAHAMS and L. E. EKSTROM, *Acta Metall.* **8** (1960) 654.
45. G. ARLT and P. QUADRIFLIEG, *Phys. Status Solidi* **25** (1968) 323.
46. D. BERLINCOURT, H. JAFFE and L. R. SHIOZAWA, *Phys. Rev.* **129** (1963) 1009.
47. S. B. AUSTERMAN, D. A. BERLINCOURT and H. H. A. KRUEGER, *J. Appl. Phys.* **34** (1963) 339.
48. L. L. CHANG, *Solid State Electron.* **10** (1967) 69.
49. L. W. JAMES, G. A. ANTYPAS, J. EDGECUMBE, R. L. MOON and R. L. BELL, *J. Appl. Phys.* **42** (1971) 4976.
50. E. SIRTL and A. ADLER, *Z. Metallkde* **52** (1961) 529.
51. G. H. OLSEN, M. S. ABRAHAMS and T. J. ZAMEROWSKI, *J. Electrochem. Soc.* **121** (1974) 1650.
52. Y. TARUI, Y. KOMIYA and Y. HARADA, *ibid.* **118** (1971) 118.
53. W. Y. LUM and A. R. CLAWSON, *J. Appl. Phys.* **50** (1979) 5296.
54. S. N. G. CHU, C. M. JODLAUK and W. D. JOHNSTON, *J. Electrochem. Soc.* **130** (1983) 2398.
55. D. B. HOLT and R. C. POND, *J. Mater. Sci.*, to be published.
56. K. DUROSE, Ph.D. thesis, Durham University (1987).
57. K. DUROSE, G. J. RUSSELL and J. WOODS, in "Microscopy of Semiconducting Materials 1985", Conference Series no. 76, edited by A. G. Cullis and D. B. Holt (Institute of Physics, Bristol, 1985) pp. 233–8.
58. F. C. FRANK, in "Metal Surfaces: Structure, Energetics and Kinetics", ASM 1962 Seminar (American Society for Metals, Metals Park, Ohio, 1963) Ch. 1, p. 1.
59. R. C. POND, in "Polycrystalline Semiconductors", edited by G. Harbeke (Springer-Verlag, Berlin, 1985) pp. 27–45.
60. F. C. FRANK, personal communication.
61. R. C. SANGSTER, in "Semiconducting Compounds", Vol. 1, Preparation and Properties of III–V Compounds, edited by R. K. Willardson and A. C. Beer (Reinhold, New York, 1962) p. 241.

Received 15 June
and accepted 27 August 1987